Photocatalytic Properties and ^{121}Sb Mössbauer Spectra of Antimonic Acid Fine Nanoparticles Prepared by Soft Chemical Solution Process

Junhu Wang,*,† Kiyoshi Ozawa,‡ Masashi Takahashi,§ Masuo Takeda,§ and Toru Nonami†

School of Life System Science and Technology, Chukyo University, 101 Tokodachi, Kaizu-cho, Toyota 470-0393, Japan, National Institute for Materials Science, 1-2-1, Sengen, Tsukuba 303-0047, Japan, and Department of Chemistry, Faculty of Science, Toho University, 2-2-1 Miyama, Funabashi, Chiba 274-8510, Japan

Received November 11, 2005. Revised Manuscript Received January 30, 2006

Two kinds of dispersed nanoparticle photocatalysts of antimonic acid, $HSbO_3 \cdot nH_2O$, namely, SbI and SbII, were prepared separately by the direct reactions of an aqueous H_2O_2 solution with Sb alkoxide complex, $Sb(O\text{-}i\text{-}C_3H_7)_3$ and metallic Sb powder according to a soft chemical solution process. Their photocatalytic properties were evaluated from methylene blue (MB, $C_{16}H_{18}N_3SCl$) degradation. SbI showed very strong adsorption capability and high photocatalytic activity under UV light irradiation. The average rates of MB degradation were estimated to be 2.403×10^{-5} m mol h^{-1} for SbI and 4.01×10^{-6} m mol h^{-1} for SbII. To investigate the reason for their difference in photocatalytic MB degradation, the two Sb-based photocatalysts were characterized by ^{121}Sb Mössbauer spectroscopy in connection with powder X-ray diffraction and photoabsorption property measurement. The lattice parameters, particle sizes, and relative surface areas were estimated to be 10.372(3) Å, 35 nm, and 43.5 m^2 g^{-1} for SbI and 10.362(4) Å, 70 nm, and 31.4 m^2 g^{-1} for SbII, respectively. Valuable information was obtained on valence state and coordination structure of Sb contained in them. These results revealed that SbI had the advantages of high dispersion, fine crystallinity, and large relative surface area as well as only containing the octahedrally coordinated Sb^{5+} species with d^{10} electronic configuration, resulting in having the high photocatalytic activity for MB degradation under UV light irradiation. A small amount of Sb^{3+} species with d^8 electronic configuration should be considered to be the main reason the photocatalytic performance of SbII for MB degradation was definitely lower than that of SbI.

Introduction

It has been well-known that preventing the recombination of photoinduced electrons and holes is very important for improving the photocatalytic activity of a semiconductor oxide photocatalyst essentially.[1−3] Some studies have proved that the photoinduced electrons and holes can be separated efficiently when the crystallinity of the semiconductor oxide photocatalyst is fine enough and the particle size is nanoscale.[4] In addition, the photocatalytic reaction mechanisms proposed up to the present suggest that preliminary adsorption of the organic pollutants on the catalyst surface is a prerequisite for highly efficient photo-oxidation.[5] Because the well-known TiO_2 photocatalyst has weak adsorption capability to most organic pollutants in general, the nanocomposite materials of TiO_2 with an absorbent, such as apatite and activated carbon, have been investigated widely and developed into an application in environmental purification.[6−8] We are interested in developing a novel semiconductor oxide photocatalyst with not only strong adsorption capability but also high photo-oxidation ability to organic pollutants. In this paper, it is reported that two kinds of well-dispersed nanoparticle photocatalysts of antimonic acid, $HSbO_3 \cdot nH_2O$ (hereafter called SbI and SbII), prepared by a soft chemical solution process show strong adsorption capability and high photocatalytic activity for degradation of methylene blue (MB, $C_{16}H_{18}N_3SCl$) dye. To provide a reasonable explanation for their difference in photocatalytic performance for MB degradation, ^{121}Sb Mössbauer spectroscopy was applied for investigating their coordination structure and valence state of Sb in connection with powder X-ray diffraction (XRD) and photoabsorption property measurement. In conclusion, the high photocatalytic activity of SbI for MB degradation should be related to its high dispersion, fine crystallinity, and large relative surface area as well as it containing only the octahedrally coordinated Sb^{5+} species with d^{10} electronic configuration. Only Sb^{5+} species with d^{10} electronic configuration, or no Sb^{3+} species with d^8 electronic

* Corresponding author. Tel: +81-565-46-1211 (ext. 6839). Fax: +81-565-46-1299. E-mail: wangjh@life.chukyo-u.ac.jp.
† Chukyo University.
‡ National Institute for Materials Science.
§ Toho University.

(1) Honda, K.; Fujishima, A. *Nature* **1972**, *238*, 37.
(2) Asahi, R.; Morikawa, T.; Ohwaki, T.; Aoki, K.; Taga, Y. *Science* **2001**, *293*, 269.
(3) Zou, Z.; Ye, J.; Sayama, K.; Arakawa, H. *Nature* **2001**, *414*, 625.
(4) Ohno, T.; Sarukawa, K.; Matsumura, M. *New J. Chem.* **2002**, *26*, 1167.
(5) Qu, P.; Zhao, J.; Shen, T.; Hidaka, H. *J. Photochem. Photobiol. A: Chem.* **1998**, *129*, 257.
(6) Tsumura, T.; Kojitani, N.; Izumi, I.; Iwashita, N.; Toyota, M.; Inagaki, M. *J. Mater. Chem.* **2002**, *12*, 1391.
(7) Nonami, T.; Taoda, H.; Hue, N. T.; Watanabe, E.; Iseda, K.; Tazawa, M.; Fukaya, M. *Mater. Res. Bull.* **1998**, *33*, 125.
(8) Nonami, T.; Hase, H.; Funakoshi, K. *Catal. Today* **2004**, *96*, 113.

10.1021/cm052487m CCC: $33.50
Published on Web 03/29/2006

configuration, existing in SbI should be considered to be the main reason the photocatalytic activity to MB degradation was clearly different between SbI and SbII.

Expermental Section

Preparation of Materials. SbI and SbII were prepared separately by a conventional soft chemical solution process reported by Ozawa et al.[9,10] An aqueous hydrogen peroxide (H_2O_2, 35%) solution and a solution of a small amount of 2-ethoxy-ethanol ($C_2H_5OCH_2CH_2OH$, >99%, Aldrich) and weighted antimony alkoxide complex, $Sb(O\text{-}i\text{-}C_3H_7)_3$ (>99.9%, Kojundo), for SbI or weighted antimony metal powder (>99.5%, Wako) for SbII were homogeneously mixed. The two mixed solutions were boiled separately for about 4 h and then several pieces of platinum foils were added to remove the excess hydrogen peroxide. Finally, the two aqueous solutions were evaporated separately and the residue was dried at 393 K overnight and then SbI and SbII nanoparticle photocatalysts were obtained.

XRD Structural Determination, Optical Photoabsorption Spectrum, and Relative Surface Area. The crystal structures of SbI and SbII were determined by XRD. A conventional Rigaku MiniFlex diffractometer with Cu Kα radiation ($\lambda = 1.54178$ Å) was used for the measurement of their XRD patterns at room temperature. The XRD data were collected with a step scan procedure within $2\theta = 5-100°$. The lattice parameters were obtained by full-profile structure refinements of the collected powder diffraction data using the Rietveld program RIETAN 97β.[11] The photoabsorption properties of SbI and SbII were evaluated by measuring their UV−vis diffuse reflectance spectra by using an UV−vis spectrometer (U-3010, Hitachi) with $BaSO_4$ as a reference at room temperature. The relative surface areas of SbI and SbII were measured by the BET method using a surface area analyzer (Monosorb, Quantachrome) by nitrogen absorption.

^{121}Sb Mössbauer Spectrum and Photocatalytic MB Degradation. ^{121}Sb Mössbauer spectra of SbI and SbII were observed by a Wissel Mössbauer spectrometer system using a $Ca^{121m}SnO_3$ source (16 MBq) and a Ge detector; in these experiments both the source and the samples containing Sb were kept at 12 K in a cryostat incorporating a closed-cycle refrigerator.[12] Their adsorption capability and photocatalytic degradation to MB were evaluated by a similar method as reported previously.[13] MB aqueous solution (2.67×10^{-5} mmol dm^{-3}, 75 cm^3) was added into a quartz cell. Weighted SbI or SbII nanoparticles was then suspended in the MB aqueous solution by using a magnetic stirrer. The adsorption capability was observed by putting the suspension in the dark. After the dark test was done, the suspension was irradiated by a 27 W black light lamp (Sankyo Denki, FPL27BLB) with a UV light intensity of about 13.6 mW cm^{-2}. The adsorption capability and photocatalytic performance for MB degradation were judged mainly by the decrease in the absorbance of MB aqueous solution, at a wavelength of about 664 nm in connection with observing the discoloration of the MB adsorbed SbI or SbII nanoparticles filtered out from the suspension. The optical absorption spectrum of the filtrate (about 3 cm^3) was measured by a UV−vis spectrophotometer (U-3010, Hitachi) after a small amount of pipetted suspension (about 6 cm^3) was subjected to centrifugation. It is reported that sulfate should be produced if MB ($C_{16}H_{18}N_3SCl$) dye was decomposed completely.[14] The sulfate concentration of the filtrate was analyzed by an ion chromatograph (Shimadzu) after the photocatalytic reaction was finished.

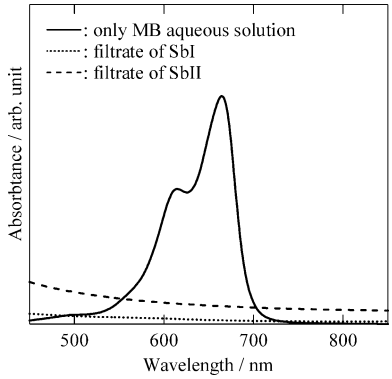

Figure 1. Absorbance variation of MB aqueous solution (2.67×10^{-5} m mol dm^{-3}) around the wavelength of 664 nm before and after the photocatalytic reactions on the SbI and SbII nanoparticles to MB degradation (MB: 75 cm^3; photocatalyst: 0.5%, 0.375 g; 27 W black light; Quartz cell).

Results and Discussion

Adsorption Capability and Photocatalytic Activity to MB Degradation. Both SbI and SbII clearly showed strong adsorption capability to MB when they were added into MB aqueous solution (2.67×10^{-5} m mol dm^{-3}, 75 cm^3), respectively. The adsorption process seemed to be very rapid. After SbI and SbII were suspended separately to MB aqueous solution for about 3 min, filtrate of near colorless (no MB absorption peak could be observed) and blue precipitate could be obtained by separating centrifugally the SbI or SbII suspension. This indicated that all of the MB was adsorbed on the surface of SbI or SbII within a very short time in the present experimental conditions. The reason was SbI and SbII suspended in MB aqueous solution were charged negatively[10] and MB is well-known as a blue cationic thiazine dye.

Figure 1 shows the absorbance variation of MB aqueous solution around the wavelength of 664 nm before and after the adsorption and photocatalytic reactions of SbI and SbII (0.5%, 0.375 g) photocatalysts. It was definite that the original absorption peak of MB around the wavelength of 664 nm disappeared completely in either case. In connection with observing the discoloration of SbI and SbII nanoparticles filtered out from their suspensions, the result could be that SbI and SbII had high photocatalytic activity for MB degradation under black light lamp irradiation when 0.5% of SbI and SbII were used separately as a photocatalyst. In the present experimental conditions, MB adsorbed on the surface of SbI nanoparticles could be degraded completely within 5 min and preciptate having almost the same color as the original SbI nanoparticles could be obtained if the suspention was separated centrifugally. However, complete degradation of MB adsorbed on the surface of SbII nanoparticles needed about 30 min in the same situation. Thus, photocatalytic activity for MB degradation on 0.5% of SbII was clearly lower than that of SbI, even though both of them exhibited strong adsorption capability to MB. The average

(9) Ozawa, K.; Wang, J.; Ye, J.; Sakka, Y.; Amano, M. *Chem. Mater.* **2003**, *15*, 928.
(10) Ozawa, K.; Sakka, Y.; Amano, M. *J. Sol-Gel Sci. Technol.* **2000**, *19*, 595.
(11) Izumi, F. In *The Rietveld Method*; Young, A., Ed.; Oxford University Press: Oxford, UK, 1993.
(12) Takeda, M. *Radioisotopes* **1985**, *24*, 628.
(13) Wang, J.; Nonami, T. *J. Mater. Sci.* **2004**, *39*, 6376.
(14) Mills, A.; Wang, J. *J. Photochem. Photobiol. A: Chem.* **1999**, *127*, 123.

rates of MB degradation were estimated to be 2.403×10^{-5} m mol h^{-1} for SbI and 4.01×10^{-6} m mol h^{-1} for SbII.

Moreover, MB adsorbed on the above Sb-based nanoparticles seemed to have a shielding effect to the UV light. An observation was conducted by changing the amount of SbI. When the amount of SbI suspended in the MB aqueous solution was less than 0.3%, MB could not be degraded completely, even with more than 30 min using the same light source. However, the photocatalytic MB degradation reaction became fast obviously when the amount of SbI suspended was more than 0.4%. It should be possible that the UV light could not reach efficiently the surface of the photocatalyst due to a scattering effect of the adsorbed MB. Since almost the same photocatalytic activity for MB degradation could be obtained when 0.5% and 0.6% of SbI were used separately, 0.5% of SbI was considered to be the optimum condition in the present experimental conditions.

The above photocatalytic MB degradation reactions on the two Sb-based nanoparticles were verified further by analyzing the sulfate ion concentration contained in the filtrate since the sulfate was known to be one of the main products of MB degradation.[14,15] As a result, detectable sulfate concentration was definitely confirmed to exist in the suspension in either case. The sulfate concentration was estimated to be 2.06×10^{-5} m mol dm^{-3} for SbI and 1.74×10^{-5} m mol dm^{-3} for SbII. It means that about 77% of MB (2.67×10^{-5} m mol dm^{-3}, 75 cm^3) was decomposed completely into the sulfate ions and others on SbI nanoparticles within 5 min under black light lamp irradiation. About 65% of MB (2.67×10^{-5} m mol dm^{-3}, 75 cm^3) was decomposed completely into the sulfate ions and others on SbII nanoparticles within 30 min under the same light source. The results also indicated that the two Sb-based nanoparticles performed differently in photocatalytic MB degradation under UV light irradiation. About this point, some reasonable explanations could be obtained from the results of ^{121}Sb Mössbauer spectroscopy, XRD structural analysis, and other measurements described below.

XRD Structural Analysis and ^{121}Sb Mössbauer Spectroscopy. Figure 2 shows the XRD patterns of SbI and SbII obtained in the present study. The XRD patterns indicated that SbI and SbII had fine crystallinity and were a single phase of antimonic acid, $HSbO_3 \cdot nH_2O$, with a distorted pyrochlore-type structure.[9,16] After the adsorption and photocatalytic MB degradation reactions were done, their pyrochlore structures were not changed. It means that their crystal structures are stable under UV irradiation. However, a small diffraction angle shift of SbII (about 0.14°) was observed toward the high-angle side relative to that of SbI, and the diffraction peaks of SbI were clearly broader than those of SbII as shown in Figure 3. This indicated that lattice parameters of SbI were larger than those of SbII and distortion of the SbO_6 octahedron that existed in their distorted pyrochlore-type structures was different, but the average particle size of SbI was smaller than that of SbII. The lattice parameters were determined to be 10.372(3) Å for SbI and 10.362(4) Å for SbII, and the average particle

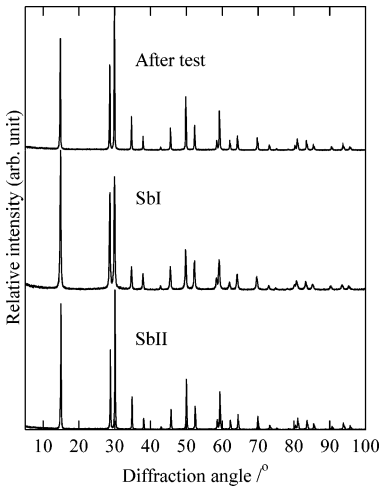

Figure 2. Powder X-ray diffraction patterns of the antimonic acid $HSbO_3 \cdot nH_2O$ nanoparticles SbI and SbII prepared by soft chemical solution process by using the starting materials of $Sb(O\text{-}i\text{-}C_3H_7)_3$ complex and Sb metal powder, respectively.

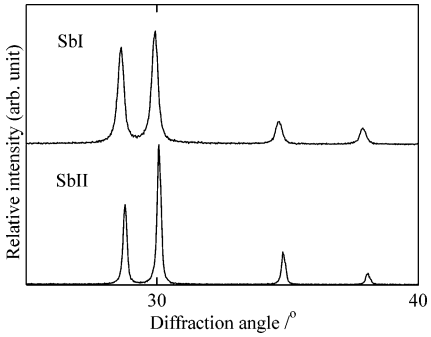

Figure 3. Expanded view of powder X-ray diffraction patterns of SbI and SbII as shown in Figure 2. Diffraction peaks of SbI are clearly broader than those of SbII.

sizes were estimated to be 35 nm for SbI and 70 nm for SbII from the line width of their diffraction peaks. The average sizes were near that of a monodispersed antimonic acid single crystal (about 50 nm) reported previously by Ozawa et al.[9] Therefore, SbI and SbII prepared in the present study should also be well-dispersed, not agglomerated, since the average particle size obtained from XRD patterns was the primary particle size.

Considering the mechanism of photocatalytic reaction, both the fine crystallinity and the high dispersion of SbI and SbII are very helpful in obtaining the efficient separation of photoinduced electrons and holes and then enhancing the photocatalytic activity. It is also possible that the difference in the distortion of the SbO_6 octahedron that exists in their distorted pyrochlore-type structures influences their photocatalytic performance. In general, distortion of the MO_6 octahedron is directly related to their various physical and chemical properties of pyrochlore-type $A_2B_2O_7$ compounds.[17−20] Wang et al. recently found that photocatalytic performance of a novel series of photocatalysts, Bi_2MTaO_7

(15) Tang, J.; Zou, Z.; Ye, J. *Chem. Phys. Lett.* **2003**, *382*, 175.
(16) Wang, J.; Zou, Z.; Ye, J. *J. Phys. Chem. Solids* **2004**, *66*, 349.
(17) Wang, J.; Nakamura, A.; Takeda, M. *Solid State Ionics* **2003**, *164*, 185.
(18) Wang, J.; Otobe, H.; Nakamura, A.; Takeda, M. *J. Solid State Chem.* **2003**, *176*, 105.
(19) Nakamura, A.; Otobe, H.; Wang, J.; Takeda, M. *J. Phys. Chem. Solids* **2005**, *66*, 356.
(20) Wang, J.; Takeda, M.; Nakamura, A. *J. Nucl. Mater.* **2005**, *340*, 33.

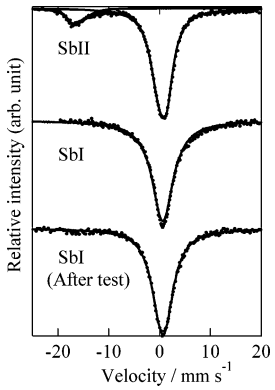

Figure 4. ^{121}Sb Mössbauer spectra for the antimonic acid $HSbO_3 \cdot nH_2O$ nanoparticles SbI and SbII at 12 K.

(M = In, Ga, and Fe), with distorted pyrochlore-type structure correlated with the distortion of MO_6 (M = In, Ga, Fe, and Ta) octahedron that existed in their structures.[16] It seemed that the photocatalytic activity became higher when the distortion of MO_6 octahedron became larger in the same distorted pyrochlore-type structure. This was probably because the driving force of the photoinduced electrons and holes became larger when the distortion of the MO_6 octahedron became larger in the same distorted pyrochlore-type structure. This point needs to be investigated further.

In addition, the relative surface areas were determined to be 43.5 $m^2\ g^{-1}$ for SbI and 31.4 $m^2\ g^{-1}$ for SbII. This also indicated that the particle size of SbI was smaller than that of SbII; also it was then possible that the active sites in the SbI surface were greater in number than those of SbII. This was also one of the possible reasons the photocatalytic activity for MB degradation on SbI was higher than that of SbII.

^{121}Sb Mössbauer spectroscopy was also used to investigate the structural properties and stability before and after the photocatalytic reaction. Figure 4 shows the ^{121}Sb Mössbauer spectra of SbI and SbII at 12 K. SbII showed two absorption peaks which were typical for Sb^{5+} (right) with d^{10} electronic configuration and Sb^{3+} (left) with d^8 electronic configuration.[12] However, SbI only showed one symmetric absorption peak which was for the Sb^{5+} species. These results indicated that a small amount of Sb^{3+} species existed in SbII, even though both of them had the same distorted pyrochlore-type structure. In addition, the Sb^{5+} species in SbI was stable before and after the photocatalytic reaction as also shown in Figure 4. This means that only the Sb^{5+} species existed in SbI, even after the photocatalytic reaction.

Figure 5 shows the UV diffuse reflection spectra of SbI and SbII. Shapes of the two spectra were slightly different from each other and the absorption band edge of SbI (about 400 nm) was shorter than that of SbII (about 450 nm). This was probably that Sb^{3+} and Sb^{5+} species coexisted in SbII and their particle sizes were different. The band gaps were estimated to be 3.10(3) eV for SbI and 2.76(2) eV for SbII from the onset of the absorption band edge. Considering the results of the RuO_2-loaded antimonate photocatalysts reported by Inoue's group,[21] the conduction and valence bands of $HSbO_3 \cdot nH_2O$ should consist of the orbitals Sb 4d and O 2p,

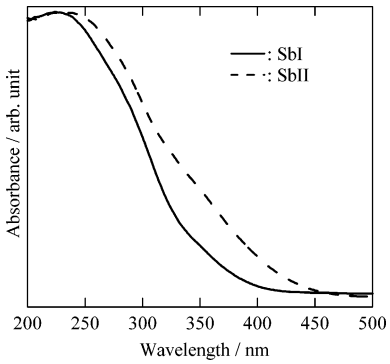

Figure 5. Diffuse reflection spectra of the antimonic acid $HSbO_3 \cdot nH_2O$ nanoparticles SbI and SbII.

respectively. Inoue et al. also pointed out that the existence of octahedrally coordinated Sb^{5+} with d^{10} electronic configuration in the RuO_2-loaded antimonate photocatalysts was very important for inducing high photocatalytic activity. As described previously, the prepared antimonic acid, $HSbO_3 \cdot nH_2O$, namely, SbI and SbII, were isostructural and had the same distorted pyrochlore-type structure. All of the Sb contained in both SbI and SbII were coordinated octahedrally by oxide ions. Thus, Sb^{3+} with d^8 electronic configuration existing in SbII should be one of the main reasons the photocatalytic activity for MB degradation on SbII was clearly lower than that of SbI under the present experimental conditions.

Conclusions

The two novel kinds of antimonic acid nanoparticle photocatalysts, $HSbO_3 \cdot nH_2O$, namely, SbI and SbII, had strong adsorption capabilities and high photcatalytic abilities for MB degradation in aqueous solution under UV light irradiation. However, the photocatalytic performance of SbI was definitely higher than that of SbII, though both of them had the same distorted pyrochlore-type structure. An explanation could be found by taking into consideration the results of ^{121}Sb Mössbauer spectroscopy, XRD structural analysis, and optical property measurement. Their strong adsorption capabilities should be due to negative charge in the aqueous solution. The high dispersion, fine crystallinity, and existence of only Sb^{5+} with d^{10} electronic configuration should be of great benefit in enhancing their photocatalytic activities. Their difference in photocatalytic performance should be from the existence of Sb^{3+} with d^8 electronic configuration and different relative surface area, particle size, and distortion of SbO_6 octahedron. The existence of Sb^{3+} with d^8 electronic configuration could be considered to be the main reason the photocatalytic performance of SbI was definitely higher than that of SbII. The results obtained in the present study would be helpful in investigating further the photocatalytic machanism of semiconductor oxide photocatalyst and developing new photocatalyst materials with highly efficient photocatalytic performance.

Acknowledgment. The reported work was finished when two of the authors (Wang and Nonami) worked at AIST (National Institute of Advanced Industrial Science and Technology, Japan) Chubu center.

CM052487M

(21) Sato, J.; Saito, N.; Nishiyama, H.; Inoue, Y. *J. Photochem. Phtobiol. A: Chem.* **2002**, *148*, 85.